

# **Water Vapor Profiles from Commercial Aircraft**

## **Report**

**January 9, 2002**

**Rex J. Fleming<sup>1</sup>, Darren R. Gallant<sup>1</sup>, Wayne Feltz<sup>2</sup>, José G. Meitín<sup>3</sup>,  
William R. Moninger<sup>4</sup>, Steven F. Williams<sup>1</sup>, and Randy T. Baker<sup>5</sup>**

1. University Corporation for Atmospheric Research
2. University of Wisconsin
3. NOAA, National Severe Storms Laboratory
4. NOAA, Forecast Systems Laboratory
5. United Parcel Service

# Water Vapor Profiles from Commercial Aircraft

Report

January 9, 2002

Rex J. Fleming<sup>1</sup>, Darren R. Gallant<sup>1</sup>, Wayne Feltz<sup>2</sup>, José G. Meitín<sup>3</sup>,  
William R. Moninger<sup>4</sup>, Steven F. Williams<sup>1</sup>, and Randy T. Baker<sup>5</sup>



A publication of the University Corporation for Atmospheric Research  
pursuant to National Oceanic and Atmospheric Administration Award No.  
NA17GP1376

- 
1. University Corporation for Atmospheric Research
  2. University of Wisconsin
  3. NOAA, National Severe Storms Laboratory
  4. NOAA, Forecast Systems Laboratory
  5. United Parcel Service

# Table of Contents

Page

<b>1. Introduction</b> .....	<b>1</b>
<b>2. Technology, Equations, and Data</b> .....	<b>3</b>
<b>3. Comparisons of Commercial Aircraft Data Versus Radiosondes</b> .....	<b>8</b>
<b>3.1 Louisville, Kentucky Comparisons</b> .....	<b>8</b>
<b>3.2 Comparisons of Opportunity</b> .....	<b>11</b>
<b>4. Moist Absolutely Unstable Layers</b> .....	<b>17</b>
<b>5. The WVSS-II and Recent Avionics Developments</b> .....	<b>22</b>
<b>6. Conclusion</b> .....	<b>27</b>
<b>Appendix 1. References</b> .....	<b>30</b>
<b>Appendix 2. Removing firmware temperature</b> .....	<b>33</b>
<b>Appendix 3. Error Evaluation</b> .....	<b>34</b>

## 1. Introduction

Accurate water vapor information is in demand for a spectrum of socio-economic applications in atmospheric science. Evans and Ducot (1994) and Fleming (1996) discussed its importance in the short-term aviation weather impacts area. Crook (1996) showed the sensitivity of convection to the vertical moisture profile, where inaccuracies in water content lead to large differences in model-predicted rainfall amounts. Lorenc et al. (1996) demonstrated the importance of accurate information of water vapor amounts in the determination of fractional cloud cover in forecasts. There are a number of water vapor issues related to climate (cf. Sun and Oort, 1995 and Lindzen, et al. 2001). Bates, et al. (1996) pointed out the value of improved in situ measurements of water vapor to help provide an absolute calibration of satellite data to provide a better climatology of upper-tropospheric water vapor. The literature contains many other references to the value of water vapor for weather and climate analysis and prediction.

Knowledge of water vapor over the four dimensions of space/time is important, but, unfortunately, its spatial and temporal variability far exceeds the current synoptic scale capability of the radiosonde network, e.g., Melfi, et al. (1989), Hanssen, et al. (1999). Moreover, the accuracy of radiosondes with respect to water vapor has always been questioned under certain conditions, e.g., Wade (1994), Wade, et al. (1993), Miloshevich, et al. (1998). Finally, water vapor is not dynamically constrained like the wind, pressure, and temperature fields (cf. Emanuel, et al., 1995), thus making it more variable and more difficult to measure properly.

Our objective in pursuing the measurement of water vapor from commercial aircraft has been to improve on the accuracy of water vapor information, and to break the synoptic scale barrier of “400-km horizontal resolution, twice a day” radiosonde coverage by ushering in a **mesoscale observing system** of water vapor, winds, and temperature. One of several motives for such an improved observing system is to help alleviate the current chaos in our National Airspace System due to excess traffic and weather delays. The Associated Press has called the summer of 2000 the “summer of aviation discontent”. FAA figures in June 2000 show 48,448 delayed flights. This was up from 41,602 delays in June 1999. Prior to 2000, the summer of 1999 was by far the worst record for delays. The Air Transport Association (ATA) says air traffic control delays in 1998 cost flyers \$1.6 billion. The ATA predicts that by 2008, there will be 43% more passengers using the airways in 2,500 more aircraft, and if things are left

unchanged, the additional traffic would result in a 250% rise in delays. Of considerable practical value is improving an understanding of the water vapor role in the evolution, movement, and decay of mesoscale convective systems. Such systems are the major cause of summertime air traffic delays. The possible implementation of this mesoscale system is described later in this report.

The timing and intensity of global warming is also tied to issues associated with water vapor. Providing detailed information from flight level tracks from various international carrier aircraft with an accurate water vapor sensor is a further motivation for this work. The importance of identifying the sharp vertical and horizontal water vapor contrasts in the Tropics has been identified by Lindzen et al. (2001).

The purpose of this paper is to describe the water vapor information obtained from two generations of water vapor measuring systems used on commercial aircraft. Section 2 describes the technology of the first generation measurement system and the data sources for comparative results shown later. Section 3 contains comparisons of water vapor profiles obtained from commercial aircraft and those obtained from two different operational radiosonde types. Section 4 reveals the ability of the commercial aircraft to capture moist absolutely unstable layers (MAULs)—as described by Bryan and Fritsch (2000). Within Sections 3 and 4, as appropriate, we show the consistency of the commercial aircraft information between different aircraft. Section 5 outlines the technology of the second-generation system for water vapor measurements from commercial aircraft, comparative results with other systems, and relevant avionics developments that impact both major and regional air carriers. This second generation system and related technology lead us to believe that we are on the threshold of implementing a composite mesoscale observing system within the United States with the commercial aircraft as the backbone of such a system. A summary of these important developments is provided in Section 6.

## 2. Technology, Equations, and Data

The history of the use of commercial aircraft as a source for atmospheric measurements is described by Fleming (1996). Also included in this reference is a discussion of the real-time digital communication system used by the air carriers. This system, called Aircraft Communication and Reporting System (ACARS), allows data to be available on the Internet in real-time—faster than radiosonde data is available. The data includes a pseudo tail number of the aircraft, time of report, latitude, longitude, winds, temperature, and water vapor.

Of the many technologies available to measure water vapor, only a very few are capable of meeting both the accuracy requirements and the day-to-day operational constraints of commercial jet aircraft. Results from two different technologies are reported in here. The first generation Water Vapor Sensing System (WVSS-I) used a thin-film capacitor to measure relative humidity (RH) directly. The second-generation Water Vapor Sensing System (WVSS-II) used a diode laser to measure the water vapor mixing ratio directly. The diode laser technology was always our first choice, but was not bid (due to its cost at that time, ca. 1994) in a competitive request for proposal. Measuring water vapor information obtained by a direct measurement of RH at **flight level** has a definite disadvantage, which we will expose immediately below. However, the application of thin-film capacitors on an aircraft also has a definite advantage over that same technology used in radiosondes.

What is unique about water vapor measurements from commercial aircraft is accounting for the aircraft's flight speed—this is critical if the water vapor sensor is measuring RH. The **total** air temperature ( $T_T$ ) measured on an aircraft equals the **static** temperature ( $T_S$ ) or ambient temperature plus the dynamic effects of the moving aircraft. The total temperature is given by

$$T_T = T_S (1 + 0.2 M^2) \quad (1)$$

where  $T$  is always in degrees Kelvin and where  $M$  is Mach number (speed of aircraft relative to the speed of sound at  $M = 1$ ). Details on this equation and on all equations related to this subject of water vapor measurements can be found in Fleming and Braune (2000). This reference and other documents related to commercial aircraft measurements can be found on the Web site:

<http://www.joss.ucar.edu/wvss/>.

The total pressure ( $P_T$ ) is similarly related to static pressure ( $P_S$ ) by:

$$P_T = P_S (1 + 0.2 M^2)^{3.5} \quad (2)$$

The most common form of relating the amount of moisture in the air is via the RH. This is defined (with respect to water, per the World Meteorological Organization) as:

$$RH = (e/e_s) 100 \quad (3)$$

where RH is a percent,  $e$  is the atmospheric vapor pressure (Pascals),  $e_s$  is the saturation vapor pressure with respect to water (Pascals);  $e_s$  is defined as saturation vapor pressure with respect to water by Fan and Whiting (1987) as:

$$e_s = 10^{[10.286T - 2148.909]/(T - 35.85)} \quad (4)$$

Another form of measurement of the water vapor content in the atmosphere (used by most meteorological prediction models) is the mixing ratio (mass of water to mass of dry air).

$$r = 0.62197e / (P - e) \quad (5)$$

where  $e$  is vapor pressure and  $P$  is pressure. Since the mixing ratio is conserved whether outside the aircraft (static environment) or within the aircraft's measurement probe (virtually identical to the total dynamic environment—see Fleming and Braune, 2000)—the water vapor mass is unchanged and the following relation holds:

$$\frac{e_{static}}{e_{probe}} = \frac{P_{static}}{P_{probe}} \quad (6)$$

where the subscript static refers to ambient conditions and the subscript probe refers to values in the probe. It can be shown that combining Eq. (6) with the definition of RH, Eq. (3), leads to

$$RH_{static} = RH_{probe} \left[ \frac{e_{s, probe}}{e_{s, static}} \right] \left[ \frac{P_{static}}{P_{probe}} \right] \quad (7)$$

The impact of Eq. (7) is primarily felt at “flight level” where the Mach number is high (~0.8) and it has relatively little impact on “ascent” and “descent” where Mach numbers are much lower (~0.2–0.4). Figure 1 is a plot of Eq. (7) where the ratio of  $RH_{\text{static}}$  to  $RH_{\text{probe}}$  is shown as a function of Mach number and temperature. One can see from the figure that for high Mach numbers and very cold temperatures, this ratio becomes substantial. This “Mach number effect” is due to the highly nonlinear nature of Eq. (4) and the effects of dynamic heating through Eqs. (1) and (2). A numerical example of this ratio is shown below. Consider an aircraft traveling at Mach = 0.8 (approximately  $234 \text{ m/s}^{-1}$ ) with an outside air temperature of  $T_s = -60^\circ \text{ C}$  (213.15 K). Eq. (1) gives the temperature in the probe as 240.4 K and Eq. (2) gives  $P_p/P_s$  as  $1/1.524$ . Eq. (4) gives  $e_{s,s}(213.15) = 1.76$  and  $e_{s,p}(240.4) = 38.41$ . From Eq. (7) we have:

$$RH_{\text{static}}/RH_{\text{probe}} = (38.41/1.76) / (1.524) = 14.32$$

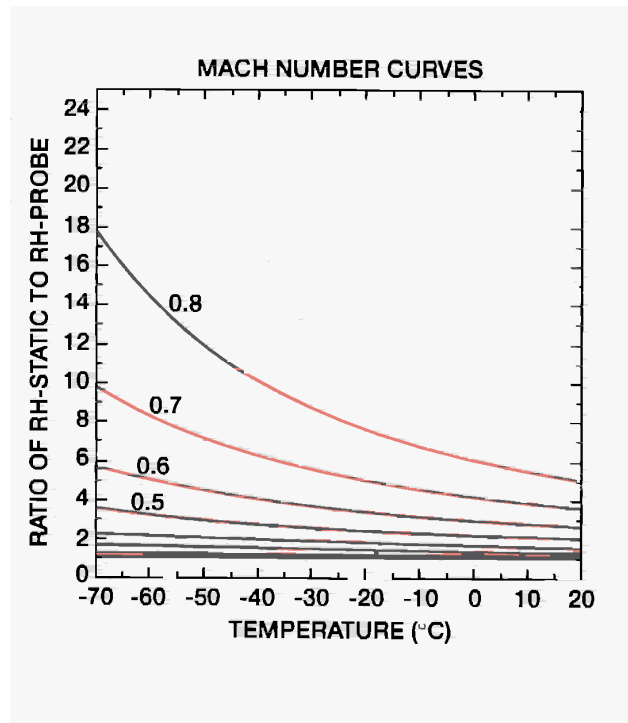


Figure 1. Ratio of  $RH_{\text{static}}$  to  $RH_{\text{probe}}$  as a function of temperature and Mach number. Mach number curves from 0.8 to 0.5 are labeled, the lower curves approach the value of 1.

In the above example there is over 27 degrees of heating due to the “Mach number effect”—dynamic heating due to the aircraft’s motion. The RH measured in the aircraft probe is thus a factor of 14 lower than the ambient RH. The software correctly accounts for the effect but

the problem is that if the RH can be calibrated at low RH values and produce a random error of only 1% of signal (which it can), then this Mach number **multiplying** effect leads to a random error of 14%. This is the bad news about measuring RH directly at flight level. On the other hand, this same dynamic heating of the aircraft's thin-film capacitor significantly improves the sensor's **response time**—providing good data in the cold upper troposphere, where Vaisala's radiosondes perform poorly in such a cold environment using a similar thin-film technology (Miloshevich, et al., 1998 and Miloshevich, et al., 2001).

There is another deficiency of thin-film capacitors over time—the accumulation over time of exposures to various gases and aerosols eventually leads to a lack of response and a dry bias in the voltage to RH response. This was seen for a time in Vaisala's packaging of radiosondes (in this case outgassing from the packaging material provided the dry bias)—Wang et al. (2001). The aircraft RH sensor is also a Vaisala product, but more robust than the technology on a low-cost radiosonde. Further, BF Goodrich Aerospace (formerly Rosemont Aerospace, manufacturer of virtually all commercial aircraft total air temperature (TAT) probes and manufacturer of the WVSS-I using a modified TAT probe) made some important changes to minimize temperature effects. Nevertheless, the exposure over time takes its toll from the aircraft operational environment, and the WVSS-I sensors eventually fail if not cleaned, recalibrated, or the sensing element replaced. Table 1 shows the month of installation and month of failure of six United Parcel Service (UPS) B-757 aircraft equipped with the WVSS-I units. The average length of service was 13 months with the range of 9–18 months.

Normally, these units would have been recalibrated after six months of flight time; however, they were left on the aircraft during the year 2000 so we were able to check their lifetime and failure mode. Monthly statistics gave a clear indication of the failure mode—excessively dry at upper levels (where the sensor is already less sensitive due to the cold temperatures) in the first month of failure, and excessively dry at all levels into the second month of failure—at this point, the data is considered worthless.

The data used in this paper includes data from those six UPS aircraft for the six month time period of July 1, 1999 to December 31, 1999. All aircraft data shown here are actual raw measurements made by the sensor (a temperature dependent software feature, similar to that used for radiosondes, was provided by Vaisala, but this was removed—see Appendix 2).

All data was gathered at a rate of 4Hz and the four samples were averaged to provide one second samples. No smoothing or filtering has been used on the data. Though the data represents one second samples, no data was recorded, so that data that we have from the six-month period is that which was transmitted by the ascent/descent formats in real-time and provided on the Internet. Over 130,000 reports (levels) of information are available for this six-month data set.

**Table 1. Longevity of WVSS-I Sensors**

<b>Pseudo Tail Number</b>	<b>Install Date</b>	<b>Stop Date</b>	<b>Comment</b>
00378	Feb. 99	Jan. 00	• 12 months good data (removed)
00376	Feb. 99	Oct. 00	• 18 months good data (5% bias wet)
00441	Feb. 99	Nov. 99	• 9 months good data
00714	April 99	March 00	• 11 months good data
00097	April 99	July 00	• 15 months good data
00375	Sept. 99	Sept. 00	• 12 months good data

### **3. Comparisons of Commercial Aircraft Data Versus Radiosondes**

Louisville, Kentucky is the main hub for UPS. While many flights with the B-757 cargo aircraft originate or terminate in Louisville, the flight track coverage of this aircraft fleet virtually covers the continental United States. There is no radiosonde site near Louisville, so a special two-week comparison test was performed in September 1999 organized by the National Weather Service (NWS) and conducted by Wayne Feltz of the University of Wisconsin. These ascent/descent profile results are discussed below in Section 3.1.

During the six-month period of 1999, there were 55 cases of comparisons of opportunity—where the aircraft ascent/descent was within 180 minutes of a sounding at one of 10 upper air stations co-located at an airport used by UPS. These ascent/descent profile results are discussed in Section 3.2. All of the data for this period has reports to 25,000 feet, but only in the two-month period of August and September of 1999 that UPS consistently supplied data in the 30,000–40,000-foot levels. Thus, this paper does not address enroute data.

#### **3.1 Louisville, Kentucky Comparisons**

The WVSS-I validation experiment was conducted from 21 September - 01 October 1999 at the Louisville International airport. The University of Wisconsin, Madison provided a suite of meteorological instruments for validation including Vaisala radiosondes, an Atmospheric Emitted Radiance Interferometer (AERI), global positioning system, Vaisala ceilometer, and a surface meteorological station. These instruments were deployed at the Kentucky Air National Guard grounds northeast of the airport terminal within a 30' long motorhome. The comparisons were conducted primarily at night—the dominant operational period of the UPS aircraft.

The Vaisala radiosondes used for this validation experiment were purchased within two weeks of manufacturing. This is important since a dry bias was known to exist within Vaisala radiosondes, has been attributed to contamination of the capacitive sensor due to outgassing of the packaging (Guichard et al. 2000; Wang et al. 2001, Turner et al. 2000). This dry bias is directly related to the amount of time the relative humidity sensor is contained within the packaging. A surface meteorological station (mounted on the motorhome) was calibrated within a calibration chamber at the University of Wisconsin - Madison's Space Science and Engineering Center (SSEC) before the deployment. Root mean square (rms) mean bias/differences between

the surface station relative humidity measurement and a one-minute average surface radiosonde relative humidity measurement were 0.38% and 1.24% respectively for the 28 radiosondes launched during the deployment. Thus, it can be concluded that there was a minimum of dry bias in the batch of sondes.

Most of the Vaisala radiosondes were launched between high frequency nocturnal UPS aircraft landing and take-off periods. About 60 UPS aircraft descended into the Louisville airport during the period (0300 - 0530 UTC) and ascended during (0700 - 0930 UTC) giving nominal radiosonde launch times of 0230 UTC, 0630 UTC, and 0930 UTC. Sondes had to be released outside of the peak flight activity. Twenty-one radiosondes were compared with ascent/descent flights of the six different B-757 cargo aircraft when the two events (aircraft ascent/descent) were within 1.5 hours of each other, providing a total of 40 comparisons. Figure 2 summarizes the rms and mean bias mixing ratio water vapor and temperature differences between the ACARS WVSS-I instrument and the Vaisala radiosondes. The results exclude flight 376 because the instrument was 5% too wet on average as compared to the other five aircraft. Figure 2 indicates a mean wet WVSS-I water vapor mixing ratio bias in the lowest two kilometers of the boundary layer as compared to the radiosondes.

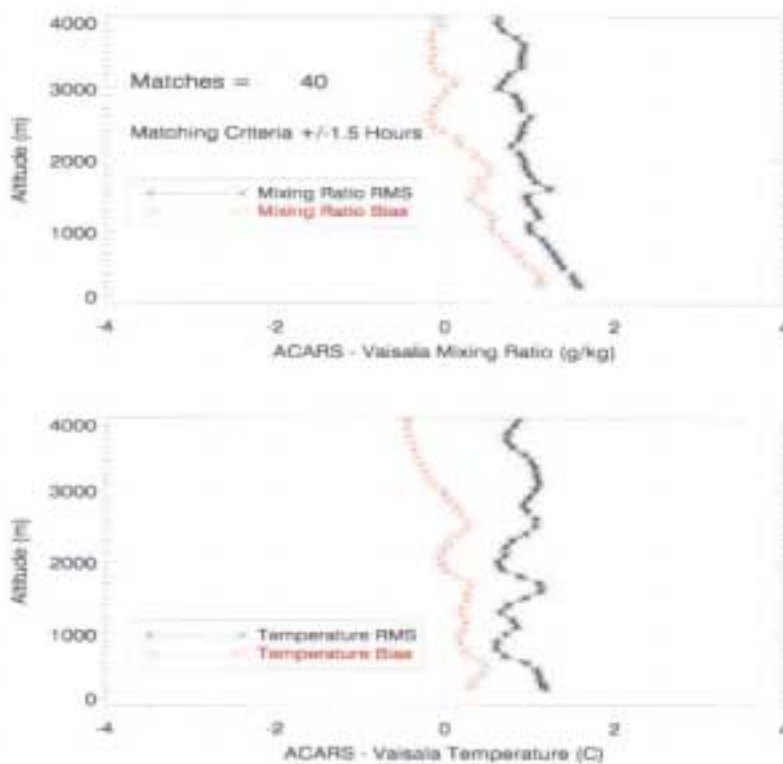


Figure 2. Water vapor and temperature rms differences and mean bias with altitude for WVSS-I compared to Vaisala radiosonde launches at the Louisville, Kentucky International airport. A match occurred when a radiosonde launch and aircraft ascent/descent were within 1.5 hours of one another.

The water vapor mean bias dropped to near 0.0 above the boundary layer. The warm temperature bias in the lowest two kilometers (shown in the lower half of Fig. 2 to range from 0.25 to 0.5 degrees) contributes to part of the wet bias. Appendix 3 indicates the effect of a warm temperature bias on the WVSS-I RH sensor values. The range of temperature bias shown above would only contribute about 0.1 g/kg to the wet bias. Thus, it is RH sensor on the aircraft itself that is biased wet compared to these Vaisala radiosonde sensors.

Figure 3 presents comparisons between the WVSS-I ascents (red/blue lines) and radiosondes (black lines) for 23 September and 24 September 1999 plotted on a Skew-T diagram. The left side of the figure shows two aircraft ascents that are 20 minutes apart. The

wet bias is apparent in both aircraft, but the pattern of change of the two aircraft and the sonde are consistent. The right side of the figure shows two aircraft descents one minute apart. Here one sees the wet bias, but also the consistency of the aircraft data being so close in time. The excessive dryness just above the boundary layer was seen in many of the Vaisala sondes during this two-week period and represents a concern that was expressed by several observers at other sites during this time period (Hal Cole and Bill Blackmore, personal communication).

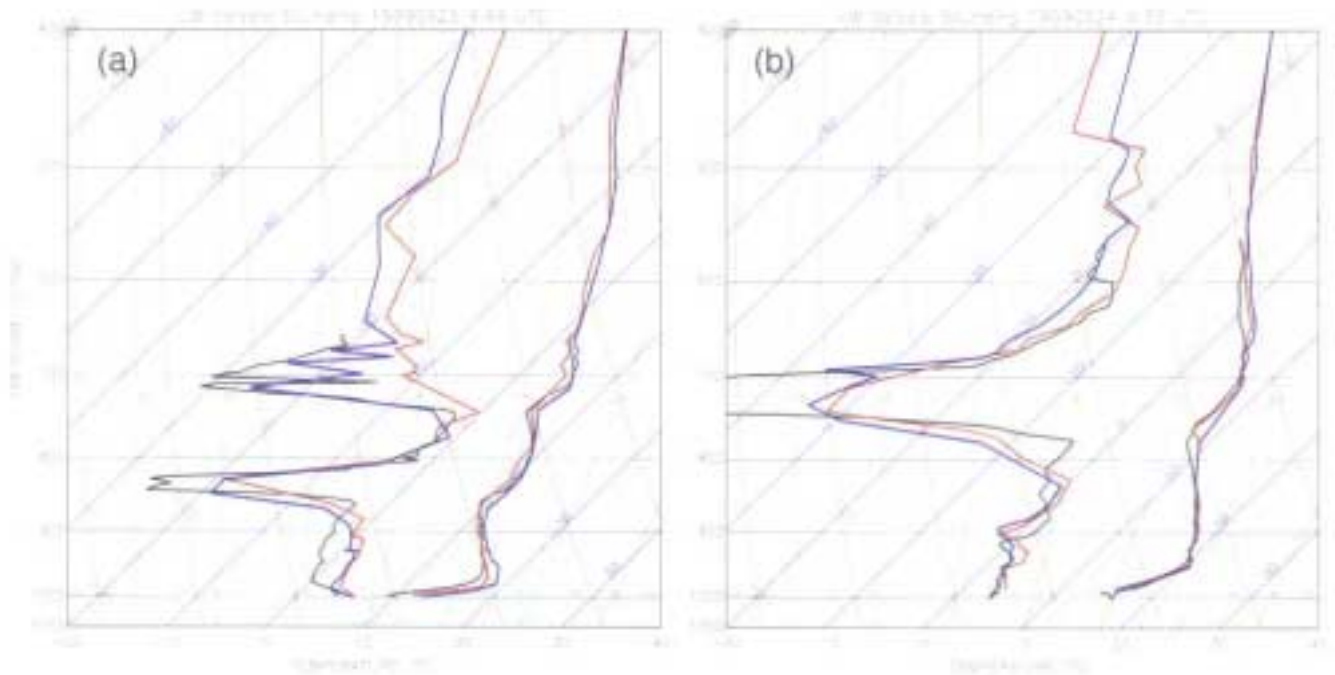


Figure 3: Left side shows Vaisala sonde (dewpoint on left, temperature on right) released at 0946 UTC 23 September 1999 (black), aircraft # 097 ascent at 0529 UTC (red), and aircraft #714 ascent at 0549 UTC (blue). Right side shows Vaisala sonde released at 0933 UTC 24 September 1999 (black), aircraft #375 descent at 0837 UTC (red), and aircraft #441 descent at 0838 UTC (blue).

### 3.2 Comparisons of Opportunity

An excellent comparison can be made between commercial aircraft data and radiosonde data when the latter have been quality-controlled by the University Corporation for Atmospheric Research (UCAR) Joint Office for Science Support (JOSS). JOSS produces high space/time quality-controlled data sets from the originally observed NWS 6-second microcomputer

Automated Radiotheodolite System (micro ART) data. These data contain information that is not routinely transmitted over the Global Telecommunications System (GTS) nor available in the National Climate Data Center’s (NCDC) unprocessed Micro ART rawinsonde data archive. Using 6-s data and the elapsed time into the ascent, an exact time and position (latitude and longitude) were determined. Details on the above process can be found in Williams et al (1993). This now gives position and time information for each point in the balloon profile similar to the commercial aircraft data, which has position and time for each point in the aircraft ascent/descent profile.

When comparing commercial aircraft data with radiosonde profiles, one must always compare pressure level to pressure level—not height to height! The aircraft “pressure/altitude” information is always actual measured pressure converted to height by a standard atmosphere equation. The radiosonde height is different! Pressure is measured as the balloon ascends, but the radiosonde height is recomputed on a second calculation pass using the hydrostatic equation with **virtual** temperature—thus water vapor effects are integrated into this balloon height. The radiosonde data were interpolated linearly with respect to the logarithm of pressure (log P) to the pressure levels at which the commercial aircraft data were reported.

There were 55 cases of colocated profiles that are summarized in Table 2.

**Table 2. Summary of colocated radiosondes and aircraft profiles**

<b>Station</b>	<b>ID</b>	<b>Sonde Type</b>	<b># of profiles</b>
Boise, Idaho	BOI	Vaisala	14
Salt Lake City, Utah	SLC	Vaisala	11
Albany, New York	ALB	VIZ	9
Oakland, California	OAK	VIZ	7
Albuquerque, New Mexico	ABQ	VIZ	6
Buffalo, New York	BUF	Vaisala	3
Shreveport, Louisiana	SHV	Vaisala	3
Jackson, Mississippi	JAN	VIZ	2

Table 3, the first of a series of Tables where the data is always shown as (Aircraft - sonde) provides a summary of all the data.

**Table 3. All data, July 1–December 31, 1999 (Aircraft-Sonde)**

DIST=distance (km) between a/c and sonde. TDIF=time difference (minutes) between a/c and sonde.

Legend Sample Size $\Delta T$ $\Delta T_d$	TDIF $\leq$ 180	TDIF $\leq$ 120	TDIF $\leq$ 102	TDIF $\leq$ 90	TDIF $\leq$ 60	TDIF $\leq$ 45	TDIF $\leq$ 30
DIST $\leq$ 50	928 0.30 4.47	867 0.35 4.31	599 0.30 2.66	505 0.36 2.37	362 0.41 2.84	303 0.40 2.70	199 0.48 2.97
DIST $\leq$ 40	850 0.29 4.28			456 0.37 2.13			181 0.49 2.7
DIST $\leq$ 30	729 0.32 3.74		488 0.31 2.49	401 0.37 2.15	299 0.42 2.52		164 0.55 2.89
DIST $\leq$ 20	603 0.31 2.94			341 0.37 1.99			138 0.54 3.00
DIST $\leq$ 10	383 0.10 1.49	363 0.13 1.54	287 0.15 1.61	240 0.37 1.36 1.53	183 0.48 1.53	170 0.49 1.37	97 0.65 2.22

The results are shown in a matrix form with the essential elements of the matrix filled in. The legend in the upper left corner of Table 3 indicates that the three variables in each matrix element are “sample size”, temperature (T) and dewpoint ( $T_d$ ), respectively. The rows give different spatial distances (in kilometers) between the aircraft report at a pressure level and the sonde report interpolated to that pressure level. These range from distances  $\leq$  50 km down to  $\leq$  10 km. One can observe from the left-most column that as the spatial separation gets smaller, the sample size falls and the dewpoint differences get smaller as one would expect.

The columns of the matrix give different temporal differences (in minutes) between the aircraft and sonde reports. These range from time differences of  $\leq$  180 minutes to  $\leq$  30 minutes. Observing the top row, we see a systematic decrease in sample size and dewpoint difference as the time separation reduces to  $\leq$  90 minutes—then a leveling off, with statistical variability as the sample size gets smaller. One sees throughout Table 3 and Table 4, the aircraft data are always wetter than the sonde data. In subsequent tables, we will concentrate on the matrix element DIST  $\leq$  50 and TDIF  $\leq$  90 and analyze these wetness differences in more detail.

Table 4 is in the same form as Table 3, but RH is replaced in the matrix of results. Notice that in Table 3, there was a **warm bias** in the aircraft temperature of approximately 0.36 K. This **increases** the calculated static RH for the aircraft. The second RH value in the matrix element (called RH' in the Table 4 legend) is the value of the calculated aircraft RH using the sonde temperature—this gives an indication of the actual wetness difference between aircraft and sonde

without the temperature bias interfering. We see a general difference of 4–5% higher RH values for the commercial aircraft as we scan down the column of TDIF  $\leq$  90 minutes.

**Table 4. All data, July 1–December 31, 1999 (Aircraft-sonde)**  
 DIST=distance (km) between a/c and sonde. TDIF=time difference (minutes) between a/c and sonde.

Legend Sample Size $\Delta$ RH $\Delta$ RH'	TDIF $\leq$ 180	TDIF $\leq$ 120	TDIF $\leq$ 102	TDIF $\leq$ 90	TDIF $\leq$ 60	TDIF $\leq$ 45	TDIF $\leq$ 30
DIST $\leq$ 50	928 8.17 7.63	867 7.48 6.69	599 6.12 5.30	505 5.47 4.61	362 6.43 5.50	303 6.15 5.22	199 7.09 5.77
DIST $\leq$ 40	850 8.05 7.49			456 5.73 4.82			181 7.11 5.70
DIST $\leq$ 30	729 7.37 6.71		488 6.59 5.66	401 6.15 5.21	299 6.56 5.53		164 7.39 5.89
DIST $\leq$ 20	603 6.42 5.72			341 5.93 4.94			138 7.28 5.66
DIST $\leq$ 10	383 4.92 4.49	363 5.16 4.53	287 5.60 4.81	240 5.43 4.37	183 5.48 4.16	170 5.23 3.80	97 6.2 4.03

Table 5 shows a comparison of results separated by aircraft versus VIZ sondes and aircraft versus Vaisala sondes. Here we have also removed the wet-biased aircraft results (#376 in Table 1, suspected to be a poor calibration from the beginning) and the dry bias aircraft (#441 in Table 1, which actually failed in November 1999)—both aircraft statistics having been included in the results heretofore. One clearly sees that the aircraft are excessively wet compared to Vaisala, but not so excessively wet compared to VIZ in all three aircraft moisture bands of comparison  $RH \geq 75\%$ ,  $46\% \leq RH < 75\%$ , and  $RH < 46\%$ . One can conclude from this and other stated information from users (Cole and Miller, 1998) and the Vaisala company itself (Vaisala, 2000) that the results give an indication of the degree of the Vaisala dry bias problem during this 1999 time period. The Vaisala Information Release indicated that the dry bias problem was reduced by 30% to 50% during this period and was only expected to be eliminated for sondes produced after May 2000. These Vaisala sondes were probably stored for a period of months and not immediately used like those discussed in Section 3.1.

**Table 5. All data except A/C #3 (biased wet, sample size = 84) and A/C #5 (biased dry, sample size = 111). (Aircraft-Sonde)**

Legend DIST ≤ 50 km TDIF ≤ 90 min.	VIZ				Vaisala			
	Sample Size	T	T <sub>d</sub> /T' <sub>d</sub>	RH	Sample Size	T	T <sub>d</sub>	RH
A/C RH ≥ 75	23	0.08	1.33 1.25	6.64	42	-0.01	3.13 3.14	16.4
46 ≤ RH < 75	50	0.24	1.92 1.70	5.23	65	0.38	3.16 2.82	9.76
A/C RH < 46	52	0.19	0.62 0.47	0.95	78	0.37	6.08 5.78	5.88

The remaining difference between the commercial aircraft dewpoints and the VIZ dewpoints indicate that the aircraft are too wet or the VIZ too dry or **both**. The argument for VIZ being slightly too dry is based upon their usual failure to reach 100% in saturated conditions as described by Schmidlin (1998). The argument for the commercial aircraft data from this WVSS-I being slightly too wet is based upon the calibration performed in the laboratory between ~0% and 70%, so that exact calibration is not assured above 70%. The net effect of **both** of these points leads to the probable conclusion that the WVSS-I data has dewpoint data about one degree too wet.

**Table 6. All data (Aircraft-Sonde) but DIST ≤ 50 km, TDIF ≤ 90 minutes**

Legend Sample Size <X>	VIZ (252)				Vaisala (253)			
	T (K)	T <sub>d</sub> (K)	Θ <sub>e</sub> (K)	RH %	T (K)	T <sub>d</sub> (K)	Θ <sub>e</sub> (K)	RH %
P ≥ 900 hPa	61 0.25	61 -0.23	61 1.27	61 1.80	51 0.36	51 2.94	51 7.16	51 12.37
P ≥ 800 hPa	48 0.06	48 0.51	48 2.53	48 3.25	87 0.58	87 4.04	87 4.56	87 7.35
P ≥ 700 hPa	68 0.64	68 0.93	68 3.16	68 1.99	45 0.33	45 4.40	45 4.30	45 8.18
P > 600 hPa	48 0.13	48 0.66	48 2.05	48 4.62	45 0.34	45 5.29	45 2.69	45 6.79
P > 400 hPa	27 0.34	27 1.20	27 1.82	27 2.16	25 0.25	25 4.92	25 1.59	25 5.66

Table 6 is a further breakdown of the VIZ and Vaisala data as a function of altitude (pressure). One sees that the Vaisala problems exist at all levels. The VIZ data are actually quite close on dewpoints except for data with pressures between 600 and 400 hPa. Also shown are equivalent potential temperature ( $\theta_e$ ) differences, which are a subject of the next section. Table 7.1 shows the mean ( $\mu$ ) difference and standard deviation of the difference ( $\sigma$ ) for all six aircraft for T,  $T_d$ , and  $\theta_e$  as well as the moment coefficient of skewness (mcs), which is defined as:

$$\text{mcs} = \tau / (\text{var})^{3/2}$$

where  $\tau$  is the third moment about the mean and  $\text{var}$  = variance is the second moment about the mean. The mcs would be zero if the error distribution were “normal”.

**Table 7.1. Aircraft – VIZ (All Data—252 Sample Comparisons, Distance  $\leq$  50 km, TDIF  $\leq$  90 min.)**

	T	$T_d$	$\theta_e$
$\mu$	0.31	0.55	2.23
$\sigma$	0.88	4.37	3.41
mcs	-0.77	0.19	-0.08

Table 7.2 is more representative as the excessively dry-biased and wet-biased aircraft (#5 and #3 respectively) have been removed.

**Table 7.2. Aircraft – VIZ (No Aircraft #3 or #5—125 Sample Comparisons, Distance  $\leq$  50 km, TDIF  $\leq$  90 min.)**

	T	$T_d$	$\theta_e$
$\mu$	0.19	1.27	2.33
$\sigma$	0.73	2.74	2.69
mcs	1.29	1.75	0.44

#### 4. Moist Absolutely Unstable Layers

The use of real-time commercial aircraft winds and temperatures in the United States continues to grow. In an earlier discussion (Fleming, 1996) the number of reports had tripled to over 22,000/day. That number has now more than tripled again as the number is over 70,000/day in the United States. The use of this commercial aircraft data in other countries is now growing at a very fast pace. The important action now is to complete this real-time data set with the addition of water vapor measurements.

Benjamin, et al. (1999) have shown the impact of these commercial aircraft data on improved predictions of winds and temperatures. Figure 4 reveals the impact of 12 hour, 6 hour, 3 hour and 1 hour forecasts—all valid at the same time—in terms of the errors as a function of pressure (height). The clear systematic improvement in the wind field is especially evident. Also quite illuminating is the complete lack of improvement in the prediction of RH—and the rather shocking value of the error in this field after only one hour of prediction.

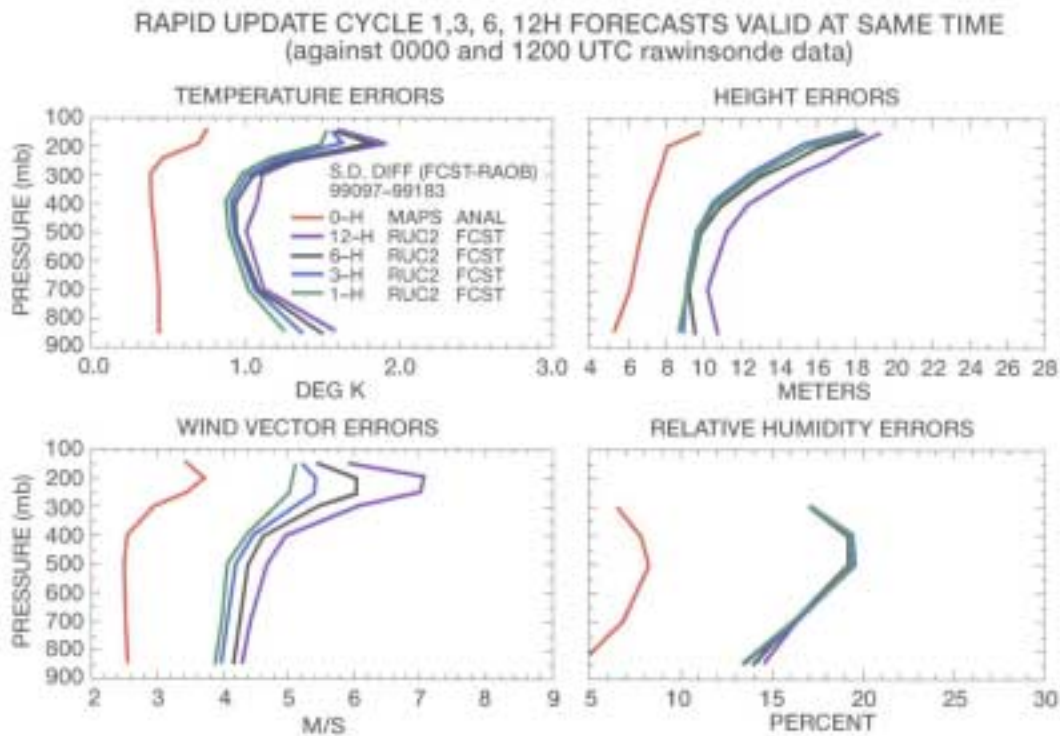


Figure 4. Rapid update cycle forecasts of 1, 3, 6, and 12 hours, all valid at the same time, provide error statistics as a function of height for the fields indicated. Provided by Stan Benjamin of the NOAA Forecast Systems Laboratory.

Those who use numerical models as guidance and have to make operational forecasts on the front line in aviation weather forecast offices or in NWS forecast offices know the need of **independent** measurements of temperature and water vapor information. In fact, an official operational assessment of the commercial aircraft data conducted by the NWS (Decker, et al, 1999) points out the forecaster’s repeated view that dewpoint measurements are needed to make ACARS data a truly complete upper air observing system. For example, those who have used thermodynamic charts know the value of the equivalent potential temperature ( $\theta_e$ ). An interesting look at  $\theta_e$  and its use in the definition of moist absolutely unstable layers (MAULs) has recently been described by Bryan and Fritsch (2000). The existence of these MAULs may shed some light on the maintenance of mesoscale convective systems. The following discussion will compare statistics on MAULs observed in the complete six-month aircraft data set with those from a much larger data set used by Bryan and Fritsch (2000) and will show a few examples of these MAULs in comparisons of opportunity.

The definition of Bryan and Fritsch (2000), hereafter (BF), is that a sounding is considered to have a MAUL if it contained a **saturated layer** in which the equivalent potential temperature ( $\theta_e$ ) **decreased** with height. The definition of  $\theta_e$  by Bolton (1980) was used and is used here in this analysis of the ability of commercial aircraft to accurately depict MAULs. Saturation was defined by BF as a dewpoint depression of  $\leq 1^\circ \text{C}$ . This criteria for saturation was chosen because of the reported accuracy of radiosonde humidity sensors (0.2–0.5°C, WMO 1996) and because of the typical dry bias at high relative humidity (Schmidlin, 1998). The same definition of saturation was used here.

Table 8. Comparison of % MAULS encountered: Aircraft (WVSS-I) and Bryan and Fritsch (2000)

	All A/C	All A/C (not #3 and #5)	Bryan and Fritsch
All MAULS	20.3%	18.1%	24.1%
MAULS with a depth > 100 hPa	9.2%	7.2%	2.4%
MAULS with depth > 100 hPa and $\delta\theta_e / \delta z \leq -3\text{K/km}$	3.8%	2.9%	1.1%

Table 8 provides a summary of the percent of aircraft profiles with MAULs and results from a similar table in BF. The first column of Table 8 shows the percent of profiles for all six aircraft over the six-month period for various categories: all MAULs, MAULs with a depth > 100 hPa, and MAULs with a depth > 100 hPa **and**  $\delta\theta_e / \delta z \leq -3\text{K/km}$ . The second column is more realistic, after removing the biased wet aircraft and the one that failed (became excessively dry) in the last two months. The third column of Table 7 represents the result of BF. Note their much larger data set—the six-month aircraft data set from six aircraft had over 130,000 reports (levels) while the BF data set (over a larger period of time) had over 130,000 complete soundings.

Before a discussion of these results, it is good to review three ways in which **apparent** (but unrealistic) MAULs can appear in radiosondes or aircraft profiles: (i) instrument error, (ii) wet or ice-covered sensors that continue reporting saturated conditions after leaving clouds or precipitation, and (iii) rapid horizontal advection of a balloon-borne sounding or an aircraft-equipped sensor through a saturated environment with a strong horizontal temperature gradient. The numbers in Table 8 for “All MAULs” (18.1% for the aircraft and 24.1% for the radiosondes) are quite close. Because of reason (ii) above, the radiosondes would have a higher number of apparent MAULs due to sensor wetting. While no aircraft probe (commercial aircraft or research aircraft) is perfect in this regard, the WVSS-I probe was aerodynamically improved to reduce such wetting—and a sensor (if wet) would dry out much faster in the aircraft case than for the slower moving sonde. Thus, both percentages are comparable and probably higher than reality.

The numbers in the other two categories in Table 8 of deep and extensive MAULs are significantly smaller for both aircraft and radiosondes, but the aircraft numbers are larger. The dominant reason for this to be true would be reason (iii) where the lengthened slant path and rapid horizontal advection of the aircraft (upon ascent or descent) through a saturated environment that could encounter horizontal temperature gradients (both for or against an indication of an apparent MAUL), which would statistically arrive at a greater number of MAULs.

We now observe individual examples of MAULs. Figures 5a and 5b show the time consistency of a MAUL over a city in Iowa on August 27, 1999 (not near a sounding site) from an aircraft descent (last report at 04:11 UTC) and later from that same aircraft’s ascent (first report four hours later at 08:08 UTC). Placing Fig. 5a over Fig. 5b indicates that the saturated layers have virtually the same values except that the depth of the MAUL has increased from 6080 feet (9150–3070) to 7160 feet (10,020–2860).

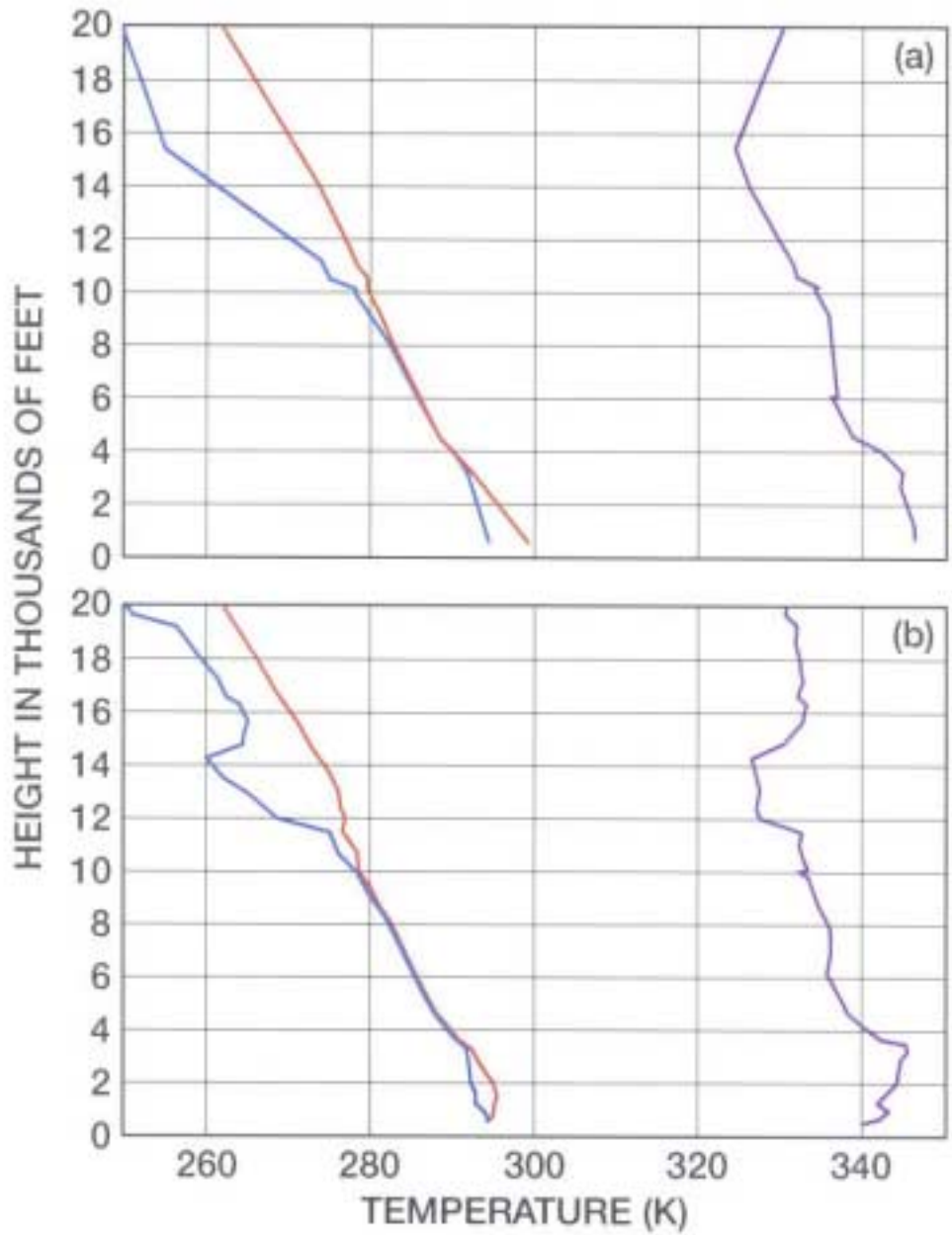


Figure 5. Thermodynamic data ( $T$ ,  $T_d$ ,  $\theta_e$ ) as function of height from aircraft #00714. (a) Descent over Iowa with last report 0411 UTC 27 August 1999. (b) Ascent over Iowa with first report 0808 UTC 27 August 1999. Temperature in red, dewpoint in blue, and  $\theta_e$  in purple.

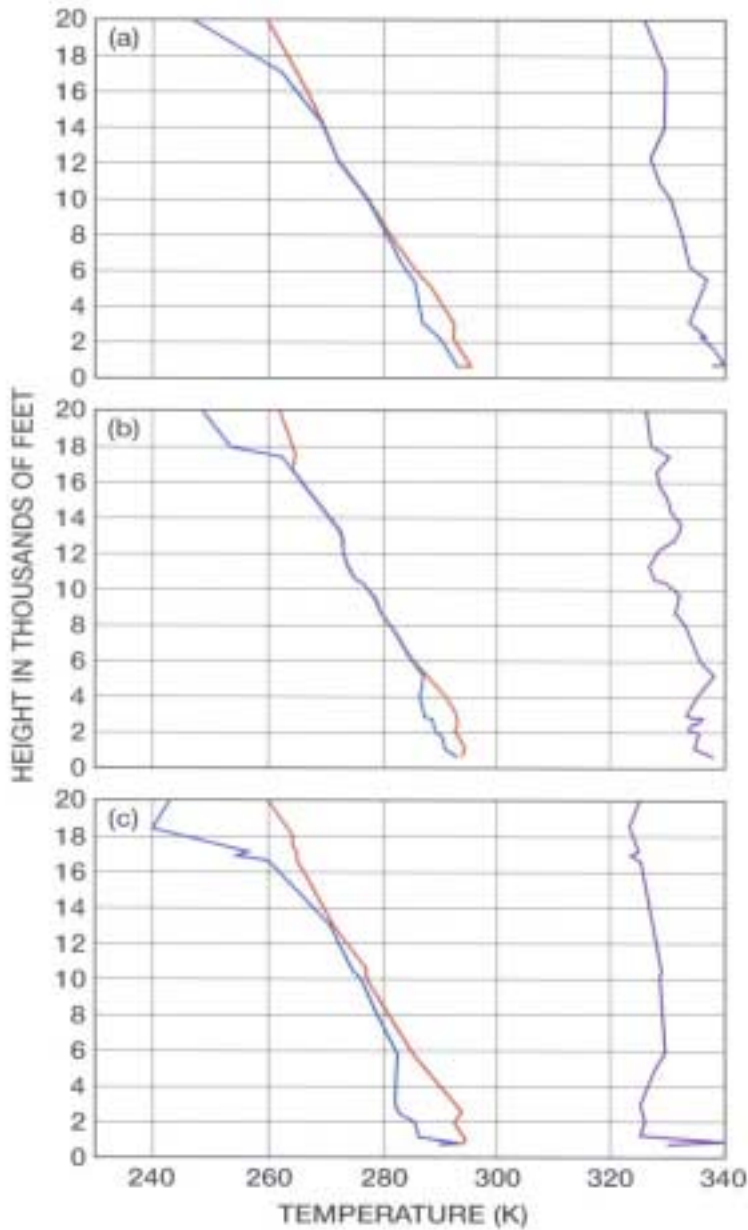


Figure 6. Thermodynamic data ( $T$ ,  $T_d$ ,  $\theta_e$ ) as a function of height. (a) Descent over BUF (0823-0841) UTC 25 August 1999 from aircraft #00097. (b) Ascent over BUF (1006-1016) UTC 25 August 1999 from aircraft #00097. (c) Radiosonde launch at BUF 1200 UTC 25 August 1999. Temperature in red, dewpoint in blue, and  $\theta_e$  in purple.

Figures 6a, 6b, and 6c compare an aircraft descent at BUF (08:23–08:41 UTC on August 28, 1999) with the same aircraft’s ascent at BUF (approximately 1.5 hours later at 10:06–10:16 UTC) and with the BUF radiosonde (approximately 1.5 hours later again at 12:00 UTC). There are minor differences between the three figures, but the consistency is unmistakable.

## 5. The WVSS-II and Recent Avionics Developments

The WVSS-I program was a proof-of-concept demonstration. It has succeeded in that capacity. It was never intended that the WVSS-I would become an operational system because it required a new probe (hence, a new aperture in the aircraft skin) over and above the TAT probe required on commercial jet aircraft. It was not intended that the measurement of RH would be carried forward as an operational measurement concept because of the limiting Mach number effect discussed earlier. When the method of choice for water vapor measurements became available at reasonable cost (the diode laser was too expensive at the time of WVSS-I procurement), a parallel development effort was initiated. The WVSS-II is significantly superior to the WVSS-I in three important ways.

(1) Accuracy: The measurement concept uses a single mode diode laser capable of fine accuracy and precision (even into the stratosphere) and represents the "standard" of water vapor measurement accuracy today.

(2) Probe replacement on aircraft: This WVSS-II probe independently measures temperature and water vapor, and is a replacement for the existing TAT probe on commercial aircraft. It fits into the same aperture, unlike the WVSS-I that fits into a larger aperture on the other side of the aircraft.

(3) Maintenance Interval: The method of implementation of the diode laser of the WVSS-II allows a maintenance interval of two+ years as opposed to the six month interval proposed for the WVSS-I.

The use of diode lasers to measure accurately the atmospheric water vapor mixing ratio has been proven on high altitude balloons and NASA research aircraft (cf. May, 1998). The measurement concept uses Beer's Law in the form:

$$I = I_0 \exp(-\sigma n l)$$

where  $I$  = laser intensity at detector

$I_0$  = laser initial intensity

$\sigma n l$  = absorbance

with  $n$  = number density of absorbing species

$l$  = optical path length

$\sigma$  = molecular absorption cross section

In the usual application of the above formula,  $I$  and  $I_0$  are measured,  $\sigma$  and  $l$  are known, thus the number density ( $n$ ) can be calculated from all the other available quantities. For increased detection sensitivity, thus higher precision and accuracy, second harmonic detection is utilized in which a small-amplitude wavelength modulation is added to the laser current (described in May, 1998 and in greater detail in May and Webster, 1993).

The measurement concept, technology, and software of the above scheme have all been proven. A UCAR contract with SpectraSensors (Randy May) to reduce the path length to a short distance inside the smallest standard TAT probe was primarily a size-reduction engineering problem. With prototypes produced from this contract, laboratory and flight tests allowed improvements to be made. Figure 7 is a result from a flight test of the WVSS-II on the NCAR C-130 in August 2000. This version is still not the final product, but one can see that the diode laser system inside the BFG TAT probe is providing virtually the same results as the diode laser “open path” system. This was mounted on the C-130 next to the diode laser “open path” system, which is now standard equipment for this aircraft.

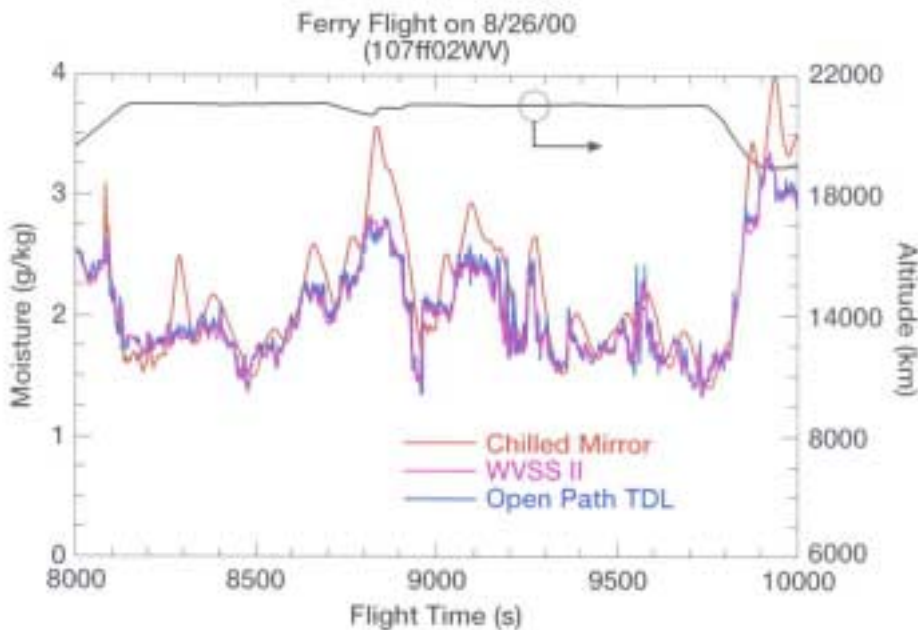


Figure 7. NCAR C-130 flight on 26 August 2000 with chilled mirror sensor, open path diode laser, and the WVSS-II. Ordinate on left marks mixing ratio (g/kg) and ordinate on right marks flight altitude (ft). Abscissa is time in seconds.

With the joining of BFG (manufacturers of 95% of the world's commercial TAT probes) and SpectraSensors, a UCAR contract was initiated to provide a new off-the-shelf TAT probe that would simultaneously and independently provide both temperature and water vapor information. This off-the-shelf product is the WVSS-II. A picture of the WVSS-II mounted next to the open path system is shown in Fig.8. The accuracy of the WVSS-II will be  $\leq 5\%$  for **all levels of the atmosphere**. See Appendix 3.



Figure 8. Picture of wing pod under the NCAR C-130 showing the “open path” diode laser (blue vertical extension in center of picture) and the WVSS-II (small probe located upper right from “open path” diode laser).

A major area of improvement as far as the air carriers are concerned is the much longer scheduled maintenance interval for the WVSS-II. The contract goal is no maintenance (recalibration) for 2+ years. The two-year period for the WVSS-II is possible for several reasons. The sensitivity of the laser receiver, the power of the diode laser, and the sensitivity of the 2<sup>nd</sup> harmonic calculation all contribute to the fact that  $I_0$  in Beer's law can degrade from 100% down to 5% and still good answers can be achieved. Such degradation can occur from actual laser power loss or from “apparent” laser power loss due to a dirty reflector inside the probe. It is this allowable degradation that suggests that the maintenance period will be 2+ years.

Satellites provide wonderful global images and horizontal and temporal information keeps improving for passively retrieved fields of information. However, the Achilles heel for the satellites is poor vertical resolution of retrieved fields—especially for water vapor in the lower troposphere and boundary layer. Current vertical resolution is about 3–4 km and even the new interferometer sounders on geostationary satellites, first described by Smith et al. (1990), which will come later in this decade, will only have 2-km vertical resolution for water vapor. This is still far from the 50–100 m vertical resolution needed for this variable in the lower troposphere and boundary layer.

Our goal of breaking the synoptic scale barrier of 400-km twice a day radiosonde profiles while at the same time achieving the high vertical resolution coverage of winds, temperature, and water vapor will require **both** the **major** air carriers and the **regional** air carriers to have the WVSS-II. The current real-time formats for downlinking winds, temperature, and water vapor allow 50-meter vertical resolution in the lower troposphere. The response time of the WVSS-II can easily accommodate this vertical resolution. All the major carriers have real-time communications. What has been missing is the real-time digital communication system on the regional air carrier aircraft.

The modern communication revolution has now solved this problem for us. Whereas the original ACARS was designed for only five specific pieces of information: time **out** from gate, **off** the runway, **on** the runway, **in** the gate (the 000I report) and “fuel on board”; this real-time communication system has evolved to include many different applications. These applications now include: Air Traffic Services (ATS—airport surface traffic monitoring and control, automatic dependent surveillance, and controller-pilot data link communications), and Airline Operation Control (AOC—aircraft monitoring (asset management), engine condition monitoring, flight plans, route planning and changes, flight monitoring, station operations (gate assignments, the 000I report and fuel on board), free text messages, and weather information.) Progress in telecommunications and avionics hardware has now brought these services to regional air carriers.

The regional air carriers with GPS receivers can now provide the needed latitude, longitude, and winds. The communications boom and the value of the above real-time information in providing the air carriers with safety, efficiency, capacity, asset management, and increased profits, has led to miniaturized avionics packages for regional carriers that can link the weather information to the next generation ACARS communication system.

Figure 9 shows coverage from the commercial aircraft system in a rectangular region in the eastern half of the country from just one major carrier and two of its subsidiary regional carriers. This coverage approaches 200 km horizontal resolution, a typical sounding frequency of 8–10 per day, and vertical resolution of 50 m. When one adds all major carriers and all regional carriers, including the nighttime package carriers, one can approach these above values in most of the continental United States except for the sparsely populated regions that have fewer airports.

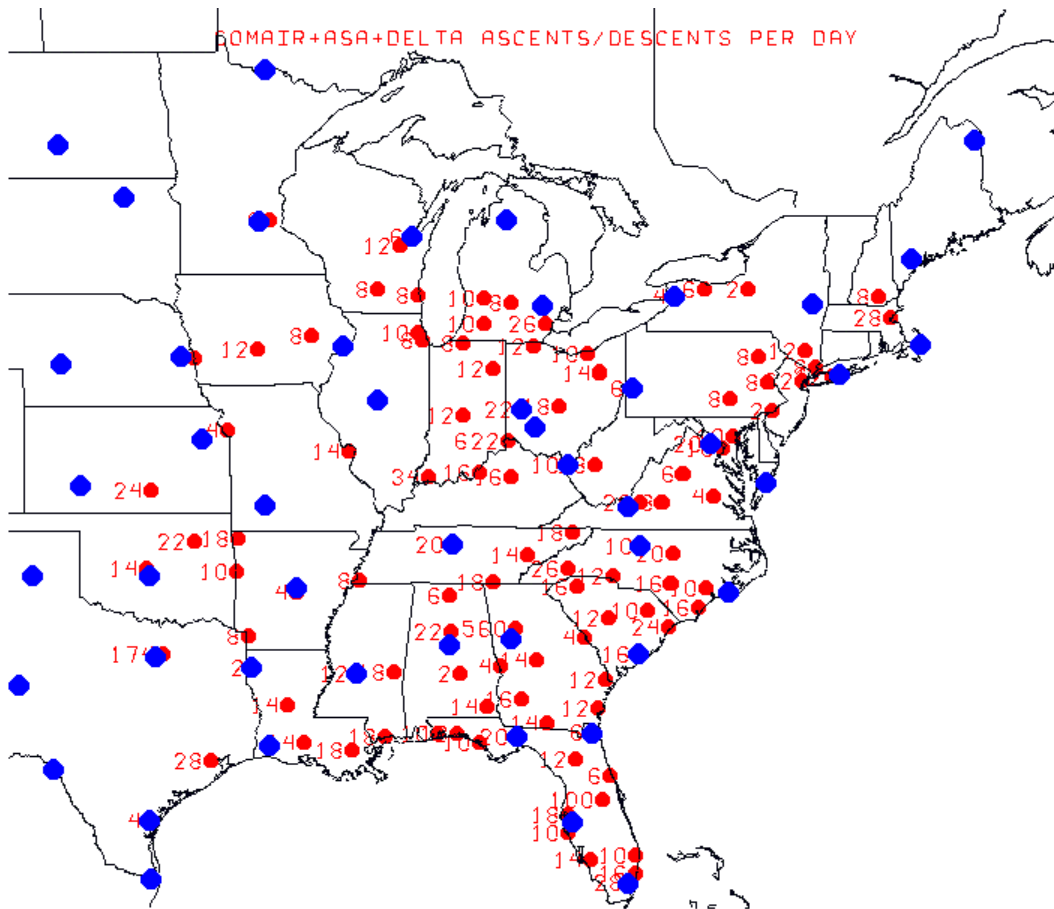


Figure 9. Sample rectangular area covering most of eastern half of the United States. Blue dots are current radiosonde site locations. Red dots show unique cities covered by just three carriers: Delta Airlines and two of its regional carriers COMAIR and Atlantic Southeast. Red numbers near red dots indicate the number of ascents and descents per day at each city—**just from these three carriers.**

## 6. Conclusion

The WVSS-I program was a proof-of-concept program. There were a number of experts who said it could not be done—and indeed, it took much longer than expected to reach a conclusion than anticipated. This was due more to procurement policies, company cultures, and working within the difficult commercial aviation environment rather than complex scientific issues. The average lifetime of the WVSS-I sensor was 13 months (without any recalibration) and the range of lifetimes for the original six UPS B-757 aircraft with Allied Signal avionics equipment was 9 to 18 months. Results shown in Section 3 reveal that the WVSS-I is competitive with radiosondes with regard to accuracy. Comparison of **all** the commercial aircraft data with the VIZ sonde indicate a 0.55 degree wet dewpoint bias of the aircraft (Table 7). Compensating for the 0.31 degree warm bias of the aircraft reduces the dewpoint bias to 0.28 degrees.

Differences between the aircraft and VIZ data are probably due to a less than accurate calibration of the aircraft data (especially at RH values above 70%) and partially due to a dry bias of VIZ near saturation values. Better calibration procedures and ongoing statistical monitoring could reduce or remove any bias in such a sensor system. While more accurate calibration procedures could be implemented for the thin-film RH sensor, this technology is simply not appropriate for jet aircraft due to the Mach number effect. Measuring dewpoint directly by chilled mirrors (which have other problems, including response time adequacy) or measuring mixing ratio directly by a diode laser (WVSS-II) avoids this Mach number effect.

The ability of the WVSS-I to depict MAULs was identified. The statistics are similar to those for radiosondes after accounting for the reasons why both are probably too high compared to nature. Examples were shown where the MAULs were consistent over time for the same aircraft and where the aircraft depiction very closely resembled that of the radiosonde.

The concept of the diode laser to measure very accurate mixing ratios was previously shown in the literature. Here it was demonstrated that this technology works within the smallest TAT probe manufactured for major and regional jet aircraft. An off-the-shelf product will be certified in 2002 and future FAA plans are to help certify this product for virtually all aircraft types. Avionics technology has evolved to allow the regional air carriers to take advantage of the real-time communications and the WVSS-II.

With the above developments, one can conceive of a national network of 200-km horizontal resolution profiles of 8–12 times per day from a commercial aircraft system. Using actual contract prices (\$20K installed) for the WVSS-II, reasonable assumptions of maintenance and communication costs over the 20-year lifetime of the unit, and typical numbers of ascent/descent (four each per day per 325 flight days per year), one arrives at a total cost of approximately \$60K for 52,000 profiles over the 20-year period or \$1.15 per profile. Assuming one can raise the capital cost from some source, we are on the threshold of a mesoscale upper air observing system for winds, temperature, and water vapor.

## **Acknowledgments**

The Federal Aviation Administration's Aviation Weather Research Program and the National Oceanic and Atmospheric Administration's Office of Global Programs supported the development of the first and second-generation water vapor sensing system for commercial aircraft described herein. The National Weather Service supported the Louisville, Kentucky evaluations through the University of Wisconsin.

## Appendix 1. References

- Bates, J. J., X. Wu, and D. L. Jackson, 1996: Interannual variability of upper-troposphere water vapor band brightness temperature. *Journal of Climate*, **9**, 427–438.
- Benjamin, S. G., J. M. Brown, K. J. Brundage, D. Kim, B. Schwartz, T. Shirmova, and T. L. Smith, 1999: Aviation forecasts from the RUC-2. Preprints, 8<sup>th</sup> Conference on Aviation, Range, and Aerospace Meteorology. Dallas, AMS, 486–490.
- Bolton, D., 1980: The computation of equivalent potential temperature. *Mon. Wea. Rev.*, **108**, 1046–1053.
- Bryan, G. H. and J. M. Fritsch, 2000: Moist absolute instability: The sixth static stability state. *Bulletin of the American Meteorological Society*, **81**, 1207–1230.
- Cole, H., and E. Miller, 1998: Correction and re-calibration of humidity data from TOGA-COARE radiosondes and development of humidity correction algorithms for Global World Climate Research Programme. *Proceedings of a Conference on the TOGA Coupled Ocean-Atmosphere Response Experiment (COARE), Boulder, Colorado, USA, 7–14 July, 1998*, WCRP-107, WMO/TD-No. **940**, 139–141.
- Crook, N.A., 1996: Sensitivity of moist convection forced by boundary layer processes to low-level thermodynamic fields. *Mon. Wea. Rev.*, **124**, 1767–1785.
- Decker, R., R. D. Mamrosh, and C. E. Weiss, 1999: ACARS operational assessment: description and interim results. Third Symposium on Integrated Observing Systems, 10–15 January, 1999, AMS, Dallas, TX, 24–27.
- Emanuel, K. and coauthors, 1995: Report of the first prospectus development team of the US Weather Research Program to NOAA and the NSF. *Bull. Amer. Meteor. Soc.*, **76**, 1194–1208.
- Evans, J.E., and E.R. Ducot, 1994: The integrated terminal weather system (ITWS). *Lincoln Lab. Journal* **7**, **2**, 449–474. [Available from Lincoln Laboratory, Massachusetts Institute of Technology, 244 Wood St., Lexington, MA 02173-9108.]
- Fan, J., and J. Whiting, 1987: Calculation and accuracy of humidity value. *Sixth Symp. Meteorological Observations and Instrumentation*, New Orleans, LA, Amer. Meteor. Soc., 237–240.
- Fleming, R. J., 1996: The use of commercial aircraft as platforms for environmental measurements. *Bull. Amer. Meteor. Soc.*, **77**, 2229–2242.

- Fleming, R. J., and C. E. Braune, 2000: Background information on the first-generation, real-time Water Vapor Sensing System for commercial aircraft, FAA Report, April 17, 2000, 33 pp.
- Guichard, F., D. Parsons, and E. Miller, 1999: Thermodynamic and radiative impact of the correction of sounding humidity bias in the tropics. *J. of Climate*, **20**, 3611-3624
- Hanssen, R. F., T. M. Weckwerth, H. A. Zebker, and R. Klees, 1999: High-resolution water vapor mapping from interferometric radar measurements. *Science*, **283**, 1297–1299.
- Heymsfield, A.J., and L.M. Miloshevich, 1995: Relative humidity and temperature influences on cirrus formation and evolution: Observations from wave clouds and FIRE-II. *J. Atmos. Sci.*, **52**, 4302-4326.
- Lindzen, R. S., M. Chou, and A. Y. Hou, 2001: Does the earth have an adaptive infrared iris? *Bull. Amer. Meteor. Soc.*, **82**, 417-432.
- Lorenc, A.C., D. Barker, R.S. Bell, B. Macpherson, and A.J. Maycock, 1996: On the use of radiosonde humidity observations in mid-latitude NWP. *Meteorol. Atmos. Phys.*, **60**, 3-17.
- May, R. D., 1998: Open-path, near-infrared tunable diode laser spectrometer for atmospheric measurements of H<sub>2</sub>O. *Journal of Geophysical Research*, **103**, 19,161–19,172.
- May, R. D. and C. R. Webster, 1993: Data processing and calibration for tunable diode laser harmonic absorption spectrometers. *J. Quant. Spectrosc. Radiat. Transfer*. **49**, 335–347.
- Melfi, S. H., D. Whiteman, and R. Ferrare, 1989: Observation of atmospheric fronts using Raman lidar moisture measurements. *J. App. Meteor.* **28**, 789–806.
- Miloshevich, L. M., A.J. Heymsfield, and S.J. Oltmans, 1998: Undermeasurement of high relative humidities in the upper troposphere by Vaisala RS80-A radiosondes. Preprints, *Tenth Symp. on Meteorological Observations & Instrumentation*, Phoenix, AZ, Amer. Meteor. Soc., 74-79.
- Miloshevich, L. M., H. Vömel, A. Paukkunan, A. J. Heymsfield, and S. J. Oltmans, 2001: Characterization and correction of relative humidity measurements from Vaisala RS80-A radiosondes at cold temperatures. *Journal of Atmospheric and Oceanic Technology*, **18**, 135–156.
- Schmidlin, F. J., 1998: Radiosonde relative humidity sensor performance: The WMO intercomparison—September 1995. Preprints, *Tenth Symp. on Meteorological Observations and Instrumentation*. Phoenix, AZ, Amer. Meteor. Soc., 68-71.
- Schwartz, B. and S. G. Benjamin, 1995: A comparison of temperature and wind measurements from ACARS-equipped aircraft and rawinsondes. *Weather and Forecasting*, **10**, 528-544.

- Smith, W. L., H. E. Revercomb, D. D. LaPorte, L. A. Sromovsky, S. Silverman, H. M. Woolf, H. B. Howell, R. O. Knuteson, and H.-L. Huang, 1990: GHIS—The GOES High resolution Interferometer Sounder. *J. Appl. Meteor.*, **29**, 1189–1204.
- Sun, D. Z., and A. H. Oort, 1995: Humidity-temperature relationships in the tropical troposphere. *Journal of Climate*, **8**, 1974–1987.
- Turner, D. D., W. F. Feltz, and R. A. Ferrare, 2000: Continuous Water Profiles from Operational Ground-based Active and Passive Remote Sensors. *Bull. Amer. Meteor. Soc.*, **81**, 1301-1317.
- Vaisala, 2000: Contamination protection of humidity sensors in RS80 series radiosondes. *Information Release, R637en 2000-05*. Available from [www.vaisala.com](http://www.vaisala.com) upon request.
- Wade, C.G. and B. Schwartz, 1993: Radiosonde humidity observations near saturation. Preprints, *Eighth Symp. on Meteorological Observations and Instrumentation*, Anaheim, CA, Amer. Meteor. Soc., 44-49.
- Wade, C.G., 1994: An evaluation of problems affecting measurement of low relative humidity on United States radiosonde. *J. Atm. And Oceanic Tech.*, **11**, 687-700.
- Wang, J., H. L. Cole, and D. J. Carlson, 2001: Water vapor variability in the tropical western Pacific from a 20-year period of radiosonde data. *Advances in Atmospheric Science*, **18**, 752-766.
- Williams, S. F., C. G. Wade, and C. Morel, 1993: A Comparison of high resolution radiosonde winds: 6-second MICRO-ART winds versus 10-second CLASS LORAN winds. Preprints, *Eighth Symp. on Meteorological Observations and Instrumentation*, Anaheim, CA, Amer. Meteor. Soc., 60-65.
- World Meteorological Organization, 1996: Guide to meteorological instruments and methods of observations, 6<sup>th</sup> ed. WMO.

## Appendix 2. Removing firmware temperature corrections for Allied Signal WVSS-I units

The original six WVSS-I prototype units had Allied Signal avionics equipment and a Vaisala supplied software “temperature correction” code. This code is similar to their internal code used for radiosondes to handle the nonlinear effects at cold temperatures. This artificially raises the RH values in radiosondes and in the aircraft applications described here (clearly identified in histograms of the data at cold temperatures) and was removed. The effect of the removal from the Allied Signal units was to produce data as it was **actually measured** on the aircraft. Subsequent data from the Teledyne avionics on UPS aircraft equipped with the WVSS-I in 2001 never had this software feature included. The removal of the software from the firmware had to be accomplished on the ground as is described below. Further details can be found in Fleming and Braune (2000).

Mixing ratio is downlinked from the Allied Signal aircraft and the formula used can be derived from Eqs. (3) and (5) to yield:

$$r = \frac{0.62197 (RH_{probe})(e_{s,probe})}{100(P_{probe}) - (RH_{probe})(e_{s,probe})} \quad (2.1)$$

With the downlinked  $T_s$ ,  $P_s$ , and  $r$ , one can recreate the  $RH_{probe}$  value if one has the Mach number. The  $RH_{probe}$  value can then be “decorrected” from the known Vaisala “temperature correction” to come up with the original **measured** RH value in the probe. With this measured value, Eq. (2.1) then gives the proper mixing ratio  $r$ . Mach number was not available in the downlinked ascent/descent data so that an estimate of its value was provided by Randy Baker of UPS as

$$M = 0.2 + 0.61 (HGT/30,000)$$

for HGT = height in feet and

$$M = 0.81 \text{ for } HGT > 30,000 \text{ feet.}$$

The impact of the temperature correction is greater at colder temperatures. An example for  $T = 260\text{K}$  ( $\sim -13^\circ\text{C}$ ),  $P_s = 800\text{hPa}$ , and mixing ratio of  $r = 1.2\text{g/kg}$  gives an RH of 70%. Removing the “temperature correction” gave a new RH of 65%. An uncertainty analysis of Mach number values leads to final errors in the actual values of  $r$  to  $< \pm 0.5\%$  of signal for the ascent/descent data shown here.

### Appendix 3. Error Evaluation

One of the limitations we face in atmospheric science is the definition of relative humidity (RH)

$$RH = (e/e_s)(100) \quad (3.1)$$

and its susceptibility to uncertainties in temperature (T) due to the nonlinear nature of the saturation vapor pressure ( $e_s$ ) dependence upon T. This affects applications, modeling, observations on radiosondes, and observations on aircraft if we measure RH directly. Thus, the problem is certainly not unique to aircraft measurements.

The absolute error in RH ( $\Delta RH$ ) given a known value of e and an uncertainty in T ( $\Delta T$ ) is given by

$$\begin{aligned} ABS(\Delta RH) &= ABS \left( \frac{\delta RH}{\delta e_s} \quad \frac{\delta e_s}{\delta T} \right) \Delta T \\ &= ABS(-100e/e_s^2) \left( \frac{\delta e_s}{\delta T} \right) \Delta T \end{aligned}$$

If we further define the error as “error as a percent of signal” (%R), then:

$$\%R = ABS(\Delta RH/RH)(100)$$

$$\%R = (100/e_s) \left( \frac{\delta e_s}{\delta T} \right) \Delta T \quad (3.2)$$

Using the definition  $e_s$  from Fan and Whiting (1987), repeated from Eq. (4) in Section 2, we have:

$$e_s = 10^{[10.286T - 2148.909]/(T - 35.85)} \quad (3.3)$$

$$\frac{\delta e_s}{\delta T} = (e_s)(\log_e 10)[1780.156 / (T - 35.85)^2]$$

therefore, putting this in Eq. (3.2) gives:

$$\begin{aligned} \%R &= (100)(\log_e 10)[1780.156 / (T - 35.85)^2] \Delta T \\ &= 409,896.07 \Delta T / (T - 35.85)^2 \end{aligned} \quad (3.4)$$

Table 1 shows %R for various values of  $\Delta T$  over the range  $T = 243.15\text{K}$  ( $-30^\circ\text{C}$ ) to  $T = 303.15\text{K}$  ( $+30^\circ\text{C}$ ). The first column for  $\Delta T$  is the standard deviation of the difference ( $0.59\text{K}$ ) between aircraft and radiosonde found by Schwartz and Benjamin (1995), the second column value ( $0.88\text{K}$ ) is the same value from our earlier Table (6), and the third column is for  $\Delta T = 1\text{K}$ . Thus, using  $T = 283.15$  ( $10^\circ\text{C}$ ) and  $\Delta T = 1\text{K}$ , the **actual**  $\Delta\text{RH}$  is **6.7%** for  $\text{RH} = 100\%$ , **3.35%** for  $\text{RH} = 50\%$ , and **0.67%** for  $\text{RH} = 1\%$ .

Most radiosonde water vapor measurements today have evolved into using sensors that measure RH directly. This is unfortunate for several reasons besides the sensitivity due to temperature. At the cold temperatures of the upper troposphere, these sensors lose sensitivity and artificial means of raising the RH values higher have been employed (unfortunately, there have been undocumented changes in the “temperature correction formulas” over time, making the climate change problem difficult to assess). RH sensors are also difficult to manufacture with consistent properties—making calibration of each sensor a necessity. Also, as we have seen, this calibration changes over time. The above disadvantages of measuring RH also carry over to a commercial aircraft. However, there is the benefit of a faster response time due to the Mach number effect and a further disadvantage of higher random error at flight level due to that Mach number effect as seen in Eq. (7) and discussed earlier in the paper.

Table 1. Error as a percent of signal for a range of T and  $\Delta T$

T (°C)	0.59	0.88	1.00
-30	5.627	8.393	9.538
-20	5.121	7.639	8.680
-10	4.681	6.981	7.93
0	4.294	6.405	7.279
+10	3.954	5.898	6.702
+20	3.653	5.448	6.191
+30	3.385	5.048	5.737

All of these disadvantages can be avoided by a direct measurement of the mixing ratio with a diode laser. In this case, the error equations can be formulated as follows.

One can use the general form of the root sum square error analysis

$$Z = f(x, y) \quad \Delta Z = \left\{ \left[ \left( \frac{\delta Z}{\delta x} \right) \Delta x \right]^2 + \left[ \left( \frac{\delta Z}{\delta y} \right) \Delta y \right]^2 \right\}^{1/2}$$

for the mixing ratio (r) we have  $r = n_{\text{H}_2\text{O}} kT/P = nkT/P$ .

One arrives at the error as a percent of signal as follows

$$\begin{aligned} \Delta r/r &= \left\{ \left[ \left( \frac{\delta r}{\delta n} \right) \left( \frac{\Delta n}{r} \right) \right]^2 + \left[ \left( \frac{\delta r}{\delta T} \right) \left( \frac{\Delta T}{r} \right) \right]^2 + \left[ \left( \frac{\delta r}{\delta P} \right) \left( \frac{\Delta P}{r} \right) \right]^2 \right\}^{1/2} \\ &= \left\{ \left[ \left( \frac{kT}{P} \right) \left( \frac{\Delta n}{r} \right) \right]^2 + \left[ \left( \frac{nk}{P} \right) \left( \frac{\Delta T}{r} \right) \right]^2 + \left[ \left( \frac{-nkT}{P^2} \right) \left( \frac{\Delta P}{r} \right) \right]^2 \right\}^{1/2} \\ &= \left[ \left( \frac{\Delta n}{n} \right)^2 + \left( \frac{\Delta T}{T} \right)^2 + \left( \frac{\Delta P}{P} \right)^2 \right]^{1/2} \end{aligned}$$

We will consider typical ascent/descent conditions in the lower troposphere first. Here we have:

$$\Delta P/P = (1.0/500) = 2 \times 10^{-3}$$

$$\Delta T/T = (1.0)/260 = 3.8 \times 10^{-3}$$

$$\Delta n/n = \text{estimated } 3\% = 3.0 \times 10^{-2}$$

$$\%R = \Delta r/r(100) = 3.05\%$$

Here,  $\Delta n/n$  is very small since  $n$  is so large. However, the 3% accuracy is limited by our knowledge of the molecular absorption cross section for water vapor at the laser frequency. In the upper troposphere (assuming conditions of low RH = 10% at 40,000 ft), we have:

$$\Delta P/P = (1.0/186) = 5.4 \times 10^{-3}$$

$$\Delta T/T = (1.0/225) = 4.4 \times 10^{-3}$$

$$\Delta n/n = \text{estimated } 5\% = 5.0 \times 10^{-2}$$

$$\%R = \Delta r/r(100) = 5.05\%$$

The  $\Delta n/n$  is limited by the hardware sensitivity in the absorbance measurement. This sensitivity will be more accurately determined in the FAA performance tests during certification. Therefore, the error as a percent of signal is 3–5% for the WVSS-II. Downlinking this information in terms of a mixing ratio implies that model users of mixing ratio are receiving this level of accuracy.

Also, having measured mixing ratio, one could downlink an RH value using the static temperature ( $T_s$ ) and pressure ( $P_s$ ) on the aircraft. One would use

$$e = Pr/(r + 0.62197) \tag{3.5}$$

Eq. (3.2) for  $e_s$  and Eq. (3.1) for RH. **Even if these values of  $T_s$  and  $P_s$  are wrong**, a mixing ratio user on the ground would use these **same values**, and inversely solve the same above equations for the **actual measured mixing ratio and have the same accuracy confidence as before**.